fermentation

MDPI

Article

Synergistic Promotion of Direct Interspecies Electron Transfer by Biochar and Fe_3O_4 Nanoparticles to Enhance Methanogenesis in Anaerobic Digestion of Vegetable Waste

Hongruo Ma [1,*], Long Chen [1], Wei Guo [2], Lei Wang [2], Jian Zhang [2] and Dongting Zhang [1]

[1] Division of Rural Energy Applicable Technology Research, Gansu Natural Energy Research Institute, Lanzhou 730030, China; longchenfly2013@163.com (L.C.); zdongt1021@163.com (D.Z.)
[2] Lanzhou Xinrong Environmental Energy Engineering Technology Co., Ltd., Lanzhou 730000, China; lzxrgw@163.com (W.G.); lzxrwlyx@163.com (L.W.); lzxrzjyx@163.com (J.Z.)
* Correspondence: mahongruo@gneri.com.cn

Abstract: When vegetable waste (VW) is used as a sole substrate for anaerobic digestion (AD), the rapid accumulation of volatile fatty acids (VFAs) can impede interspecies electron transfer (IET), resulting in a relatively low biogas production rate. In this study, Chinese cabbage and cabbage were selected as the VW substrates, and four continuous stirred tank reactors (CSTRs) were employed. Different concentrations of biochar-loaded nano-Fe_3O_4(Fe_3O_4@BC) (100 mg/L, 200 mg/L, 300 mg/L) were added, and the organic loading rate (OLR) was gradually increased during the AD process. The changes in biogas production rate, VFAs, and microbial community structure in the fermentation tanks were analyzed to identify the optimal dosage of Fe_3O_4@BC and the maximum OLR. The results indicated that at the maximum OLR of 3.715 g (VS)/L·d, the addition of 200 mg/L of Fe_3O_4@BC most effectively promoted an increase in the biogas production rate and reduced the accumulation of VFAs compared to the other treatments. Under these conditions, the biogas production rate reached 0.658 L/g (VS). Furthermore, the addition of Fe_3O_4@BC enhanced both the diversity and abundance of bacteria and archaea. At the genus level, the abundance of *Christensenellaceae*_R-7_group, *Sphaerochaeta*, and the archaeal genus *Thermovirga* was notably increased.

Keywords: vegetable waste; anaerobic fermentation; biochar loaded with Nano-Fe_3O_4 particles; direct interspecies electron transfer

check for updates

Citation: Ma, H.; Chen, L.; Guo, W.; Wang, L.; Zhang, J.; Zhang, D. Synergistic Promotion of Direct Interspecies Electron Transfer by Biochar and Fe_3O_4 Nanoparticles to Enhance Methanogenesis in Anaerobic Digestion of Vegetable Waste. *Fermentation* **2024**, *10*, 656. https://doi.org/10.3390/fermentation10120656

Academic Editor: Giulia Bozzano

Received: 11 November 2024
Revised: 3 December 2024
Accepted: 12 December 2024
Published: 18 December 2024

Copyright: © 2024 by the authors. Licensee MDPI, Basel, Switzerland. This article is an open access article distributed under the terms and conditions of the Creative Commons Attribution (CC BY) license (https://creativecommons.org/licenses/by/4.0/).

1. Introduction

In recent years, with the vigorous development of China's economy and society, the demand for vegetables has increased significantly, driving a corresponding rise in both the planting area and production output. According to the data from the National Bureau of Statistics of China, by 2023, the vegetable planting area in China had reached 22.43 million hectares, with total production reaching approximately 828.68 million tons [1]. However, while the vegetable planting industry is promoting China's economic development, it also brings huge challenges to the ecological environment in rural areas.

In China, significant losses occur throughout the vegetable supply chain, spanning harvest, processing, storage, transportation, packaging, and consumption. It is estimated that over 30% of vegetables are lost in the form of VW during these stages [2,3]; approximately 80% or more is buried or disposed of as household garbage [4]. The total solid content of VW typically ranges from 4% and 18%, with volatile solids accounting for more than 95%. These volatile solids primarily consist of total sugars, proteins, fats, hemicellulose, cellulose, and lignin [5]. When VW is buried and decomposed by microorganisms, it rapidly decays, promoting the growth of pathogens and the production of substantial amounts of acetic acid. This acetic acid can lower the pH value of the soil, leading to the development of uncultivable land [6,7]. If this trend continues, it could pose a serious

threat to the sustainable development of agriculture and affect future food security and ecological stability.

Due to the high water content and perishable nature of VW, its use as a single substrate for AD often leads to the accumulation of VFAs, which can cause acidification of the fermentation system [7]. Hegde [8] and Alvarez [9] have reported that relying solely on VW as a substrate for AD results in VFA buildup, lowering the system's pH and ultimately causing the failure of the digestion process. Previous research [10–12] has indicated that the OLR of VW should be limited to 3.5 g (VS)/L·d to prevent acidification during AD. To mitigate this issue, much of the research on AD of VW has focused on co-digestion, where VW is mixed with other organic materials, such as animal manure or sewage sludge. However, in large-scale vegetable production areas and near cold storage facilities, there is often a lack of large-scale farms or sewage treatment plants that can supply adequate quantities of co-digestion substrates.

A complex microbial community exists in AD, and the IET between acetogens and methanogens plays a crucial role in the methanogenesis process. Recent studies have identified three primary mechanisms of IET: interspecies hydrogen transfer (IHT), interspecies formate transfer (IFT), and direct interspecies electron transfer (DIET). Both IHT and IFT rely on hydrogen or formate as electron carriers. The IHT process (Figure 1a) involves the use of hydrogen (H_2) molecules as electron carriers to transfer electrons from organic compounds such as propionic and butyric acids to CO_2. H_2 is metabolically produced by hydrogen-producing acetogens during the breakdown of organic substrates like butyric acid, propionic acid, and ethanol, which generate both H_2 and acetic acid. Energy is usually required to be absorbed during the metabolic process. In order to facilitate the transfer of electrons, methanogens consume H_2, thereby reducing its partial pressure in the system, enabling co-metabolism between hydrogen-producing acetogens and methanogens. However, if methanogens reduce the consumption rate of H_2, the use of propionic and butyric acids is slowed, resulting in the accumulation of VFAs in the AD system. Baek et al. [11] found that the IFT process involves the oxidation of formic acid to CO_2 by formate dehydrogenase, followed by the reduction of CO_2 to methane. While H_2 has advantages in terms of its high diffusion rate and low solubility, making it more effective for short-range electron transfer, formate is generally involved in long-range electron transfer [13]. However, during the AD of VW, the acidification process is rapid, leading to the accumulation of a large amount of VFAs in the early stages. This results in a high partial pressure of H_2 and an elevated concentration of formic acid, which limits the efficiency of both IHT and IFT [14].

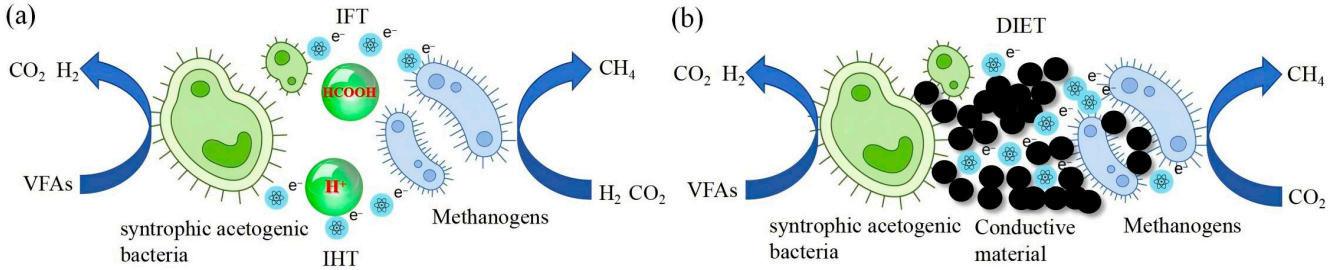

Figure 1. Schematic diagram of IET; the interspecies transfer process of IFT and IHT (**a**); the interspecies transfer process via conductive substances DIET (**b**).

DIET involves the use of conductive structures or substances to facilitate the direct transfer of electrons between microorganisms, making it a more efficient mechanism for interspecies electron transfer (Figure 1b). Unlike interspecies hydrogen transfer (IHT) and interspecies formate transfer (IFT), DIET does not require hydrolysis or acidification and allows for the direct conversion of organic matter into methane through the syntrophic metabolism of DIET-active microorganisms. This significantly improves the efficiency of anaerobic fermentation, especially in the treatment of complex organic substrates [14,15]. In 2010, Summers et al. [16] first reported the phenomenon of DIET in a co-culture system

involving *Geobacter metallireducens* and *Geobacter sulfurreducens*, discovering that the primary mode of electron transfer between these species was DIET, rather than IHT or IFT. Following this, Kato, et al. [17] demonstrated that magnetite in the co-culture system could promote DIET between *Geobacter sulfurreducens* and *Thiobacillus denitrificans*, enabling the oxidation of acetate and the reduction of nitrate to nitrite.

In the AD process of VW, the methane production rate can be enhanced by adding conductive substances to establish DIET channels. Common conductive materials used to promote DIET include carbon-based and iron-based conductive substances. Carbon-based materials, such as activated carbon, exhibit good electrical conductivity and a porous structure with a high specific surface area, providing ample space for microbial growth and favorable metabolic conditions [18]. Iron-based conductive materials, on the other hand, have been shown to influence anaerobic fermentation by regulating the secretion of extracellular polymers and promoting propionate metabolism, which in turn stimulates methane production [19]. However, the impact of the quantity of conductive substance added on the OLR and gas production rate during long-term AD of VW remains unclear. Additionally, the influence of these materials on the microbial community structure is not well understood. These questions warrant further investigation to better understand their role in optimizing AD processes.

At present, there are no reports on the use of vegetable waste as a sole substrate for AD combined with the addition of semiconductor materials to promote DIET. In this study, the synergistic properties of carbon-based and iron-based conductive materials were fully leveraged, and Fe_3O_4@BC was successfully synthesized via the co-precipitation method. This composite material was then introduced into the fermentation system to facilitate DIET. The impact of Fe_3O_4@BC on the AD of VW was thoroughly investigated. A series of AD experiments were conducted to systematically analyze the effects of different concentrations of Fe_3O_4@BC on key parameters such as OLR, gas production rate, VFAs, and microbial community structure. The goal of this study was to enhance the gas production efficiency, reduce VFA accumulation, improve the stability of the AD system, and ultimately establish a robust theoretical and practical foundation for the future engineering application and broader implementation of this approach.

2. Material and Methods

2.1. Substrate and Inoculum

The anaerobic sludge used in the experiment was from the Chengdu Biogas Science Research Institute of the Ministry of Agriculture and Rural Affairs of China. The sludge is characterized by high ammonia nitrogen content, elevated pH, and a large population of methanogens. It was further enriched and cultured in the laboratory using pig manure as the substrate. The primary characteristics of the strain are summarized in Table 1. The VW used in the experiment was sourced from Dingxi Second Branch Road Market in Chengguan District, Lanzhou City, and primarily consists of Chinese cabbage and cabbage. The VW was thoroughly washed, then pulverized into a slurry using a grinder and stored in a refrigerator at −10 °C. After mixing and pulping, the total solid (TS) concentration of the vegetable leaves was 6.95%, the volatile solid (VS) concentration was 5.16%, the soluble chemical oxygen demand (SCOD) was 2671 g/L, and the carbon-to-nitrogen ratio (C/N) was 25:1.

Table 1. Parameters of anaerobic inoculated sludge.

Parameters	TS (%)	VS (%)	pH	VFA (mg/L)	SCOD (g/L)	Ammonia Nitrogen (g/L)	C/N	The Quantity of Methanogens Individuals/mL
sludge	23.8	21.6	7.8	1990.6	2671	561.8	25:1	2.02×10^8

2.2. Anaerobic Fermentation Device and Experiment of VW

The experimental setup for AD of VW consisted of four CSTR reactors (Figure 2). The reactors were constructed from plexiglass, each having a total volume of 6 L with an effective fermentation volume of 4.5 L. Each reactor was equipped with a water bath jacket for temperature regulation, a temperature control system, a mechanical stirring device, and probes for monitoring pH and temperature. Additionally, each reactor featured a feed inlet and an outlet for sampling, with the outlet positioned at the bottom quarter of the reactor.

Figure 2. Each of the CSTR reactors used in the experiment was equipped with its own dedicated control and detection system.

The AD of VW was conducted in four CSTR reactors, respectively designated as BG; VEG.100 mg; VEG.200 mg; and VEG.300 mg. Among these, BG served as the blank control group, which did not include the addition of Fe_3O_4@BC, while VEG.100 mg, VEG.200 mg, and VEG.300 mg were the experimental groups, with Fe_3O_4@BC added at concentrations of 100 mg/L, 200 mg/L, and 300 mg/L, respectively, based on the volume of fermentation broth. The CSTRs operated under a continuous feeding fermentation process. The fermentation temperature was maintained at a constant 35 °C, with a stirring speed of 60 rpm/min. Stirring was performed every 4 h for a duration of 20 min each time.

The main steps of anaerobic fermentation were as follows (Figure 3): At the start of the experiment, 1 L of inoculum was added to each fermenter, and continuous fermentation was carried out for 7 days until gas production ceased. To prevent the rapid accumulation of VFAs in the early stage, the initial OLR of VW was set at 0.688 g (VS)/L·d (calculated based on a fermentation volume of 4.5 L). In the early phase, the OLR was increased by 20% every 3 days, with no discharge occurring during this period. Discharge was initiated only after the fermentation volume reached 4.5 L. Once the fermentation volume reached this level, the OLR was increased by 20% every 5 days, and the gas production rate was monitored. When the rate of increase in the gas production began to slow, the OLR increase rate was reduced to 10% until the gas production rate reached the maximum and started to decrease. This indicated that the system had surpassed its maximum OLR. At this point, the OLR was gradually decreased in response to changes in the gas production rate until

the system stabilized. When the gas production began to recover, the OLR was gradually increased. Once gas production began to recover, the OLR was gradually increased again. When the OLR approached 95% of the maximum OLR before acidification, the increase in OLR was halted, and the system was operated stably for more than 10 days. If there was no significant change in the gas production rate, it was concluded that the optimal OLR for the system had been reached.

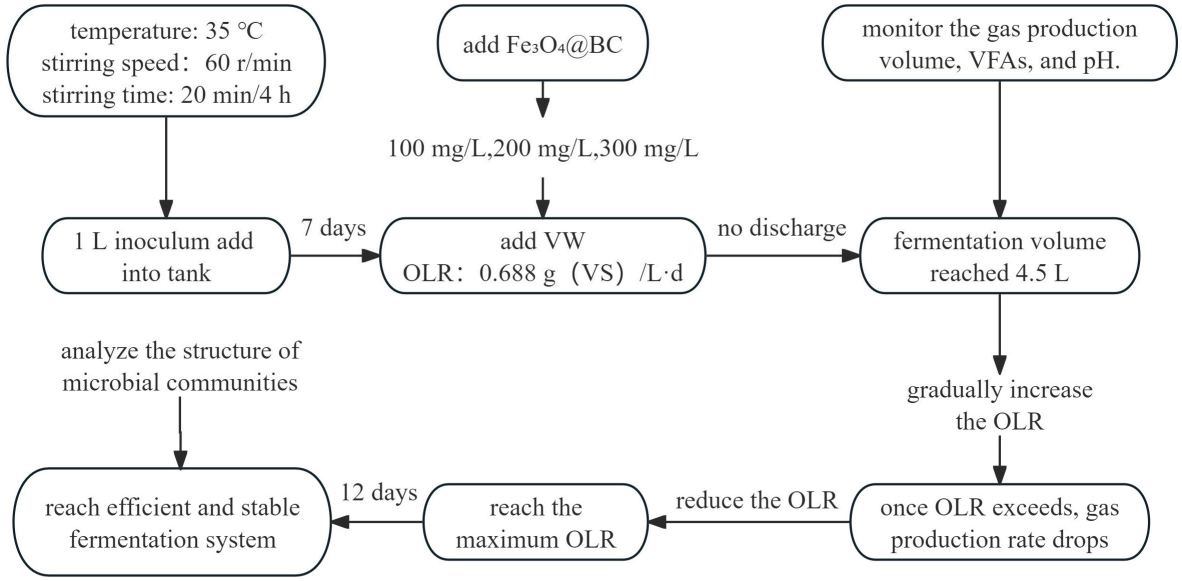

Figure 3. Research roadmap of anaerobic fermentation process.

The addition process of Fe_3O_4@BC was as follows: While the fermentation volume in the CSTR reactor was below 4.5 L, Fe_3O_4@BC was added in accordance with the daily feeding amounts. Addition of the substance ceased once the fermentation volume reached 4.5 L on the 26th day. To compensate for the loss of Fe_3O_4@BC due to discharge, the material was supplemented every 12 days thereafter. Each supplementation was calculated based on 1 L of the fermentation broth.

2.3. The Preparation Method of Fe_3O_4@BC

Fe_3O_4 nanoparticles were synthesized using the co-precipitation method. To prepare the nanoparticles, 86 mmol of $FeCl_3 \bullet 6H_2O$ and 43 mmol of $FeCl_2 \bullet 4H_2O$ were dissolved and mixed in 200 mL of distilled water. An amount of 10.00 g of BC was weighed and added to the above solution. After vigorous stirring, the mixture was allowed to precipitate for 30 min. Argon gas was then introduced to maintain stirring, and 80 mL of ammonia water was slowly added, followed by continuous stirring for an additional 30 min. The mixture was then transferred to a water bath, where Ar gas was continuously bubbled in while stirring, and the solution was heated to 90 °C for 3 h. After heating, the solution was cooled to room temperature. Subsequently, the reacted mixture was placed in a beaker, and a strong magnet was positioned at the bottom of the beaker to facilitate the precipitation of the solid phase for 10 min (Figure 4). The solid material was then washed multiple times with absolute ethanol and distilled water until the pH reached approximately 7.0. The final product, Fe_3O_4@BC, was obtained by drying the precipitate at 60 °C for 12 h.

Figure 4. The magnetic separation effect of Fe_3O_4@BC (after completely mixing the nanoparticles with water, placing a magnet at the bottom, and allowing it to stand for 5 min to observe the effect).

2.4. Analysis and Characterization Methods

The crystal structure of the samples was analyzed using an X-ray diffraction analyzer (XRD, X'Pert Pro, Philips, the Netherlands). The magnetization intensity was measured with a vibrating sample magnetometer (VSM, EV9, MicroSence, Lowell, MA, USA). The characterization of molecular structures and chemical bonds was carried out using a vacuum Fourier transform infrared spectrometer (FT-IR, Vertex 70v, Bruker, Karlsruhe, Germany). The microstructure of the samples was examined using a scanning electron microscope (SEM, Apreo, Thermo, Waltham, MA, USA). The total solids (TS) were determined by maintaining the samples at 105 °C for 2 h, while the volatile solids (VS) were tested by heating the samples at 600 °C for 2 h using a muffle furnace (MF, KDF S.90, Tokyo Rikakikai, Bunkyo City, Japan). The concentration of volatile fatty acids in biogas slurry was analyzed using a gas chromatograph (GC, 2010plus, Shimadzu, Kyoto, Japan) equipped with a wax capillary column, the detector temperature was set to 230 °C, the inlet temperature was set to 210 °C, and the column oven temperature was set to 80 °C, with a heating rate of 20 °C/min until 170 °C, followed by a 2 min retention time. The composition of the biogas was analyzed using a portable biogas analyzer (GA5000, Geotech, Chelmsford, UK). The pH was measured with an acidity meter (pH, PHS-3C, Shanghai REX, Shanghai, China), and the gas production was recorded using a wet gas flowmeter (LMF-1, Shanghai, China). For microbial community analysis, high-throughput sequencing technology was employed. Samples were collected from each fermentation tank on the 80th day of fermentation, with three parallel samples taken from each reactor. The samples were then frozen at −40 °C and sent to Beijing Novogene Company (Beijing, China) for sequencing.

To investigate the variation patterns of bacterial and archaeal community structures in the anaerobic fermentation of vegetable waste with different concentrations of Fe_3O_4@BC, this study employed high-throughput sequencing to analyze the community structures of sludge samples from the BG, VEG.100 mg, VEG.200 mg, and VEG.300 mg groups after 80 days of acclimation and cultivation. The sequencing was carried out using the Illumina high-throughput sequencing platform.

For the analysis, the V3–V4 regions of the 16S ribosomal RNA genes were amplified using universal primers (341F: CCTAYGGGRBGCASCAG and 806R: GGACTACN-

NGGGTATCTAAT). Initially, a proportion of the raw sequencing data was identified as interfering data. To ensure the accuracy and reliability of the results, the raw data of each sample were first split according to their respective barcodes, with the barcode and primer sequences removed. Subsequently, the R1 and R2 sequence data were merged using FLASH software (1.2.11). The resulting sequences were subjected to quality control to obtain clean tags, followed by chimera filtering to generate valid data for further analysis.

Operational taxonomic units (OTUs) were clustered using a similarity threshold of 97%. To evaluate the species composition and community structure across the groups, various statistical analysis methods, including *t*-test, Simper, MetagenomeSeq, LEfSe, Anosim, and MRPP, were employed to conduct significance tests. These analyses were used to identify differences in microbial communities between the experimental groups and to explore the influence of Fe_3O_4@BC addition on microbial diversity and community structure during the anaerobic fermentation process.

3. Results and Discussion

3.1. Characterization of Fe_3O_4@BC

To analyze the phase structure of Fe_3O_4 nanoparticles, X-ray diffraction (XRD) analysis was performed. As shown in Figure 5a, the relative peak intensities and positions of the samples prepared by the co-precipitation method were consistent with those of pure Fe_3O_4, exhibiting a cubic spinel structure (JCPDS No. 88-0315). No additional, irrelevant diffraction peaks were observed. Using the Debye-Scherrer equation, the grain size of the Fe_3O_4 nanoparticles synthesized by the co-precipitation method was calculated to be 18.6 nm, based on the (311) crystal plane, which showed the strongest diffraction peak. Further, vibrating sample magnetometer (VSM) analysis was conducted on the prepared Fe_3O_4@BC samples. As shown in Figure 5b, the magnetic hysteresis loop of Fe_3O_4@BC passed through the origin, with no hysteresis, residual magnetization, or coercive force, indicating that the Fe_3O_4@BC exhibits superparamagnetism at room temperature. The saturation magnetization of Fe_3O_4@BC was found to be 55.75 emu/g, which is lower than that of Fe_3O_4 with a nano-hollow sphere structure (99.033 emu/g) [20]. This decrease in saturation magnetization suggests that a significant portion of the Fe_3O_4 is encapsulated within the pores of the biochar (BC), reducing the overall magnetization of the composite. Due to the high saturation magnetization of Fe_3O_4@BC, it is possible to recover the material from the biogas slurry during the continuous anaerobic fermentation process using an electromagnet, thereby minimizing the amount of Fe_3O_4@BC required for the process.

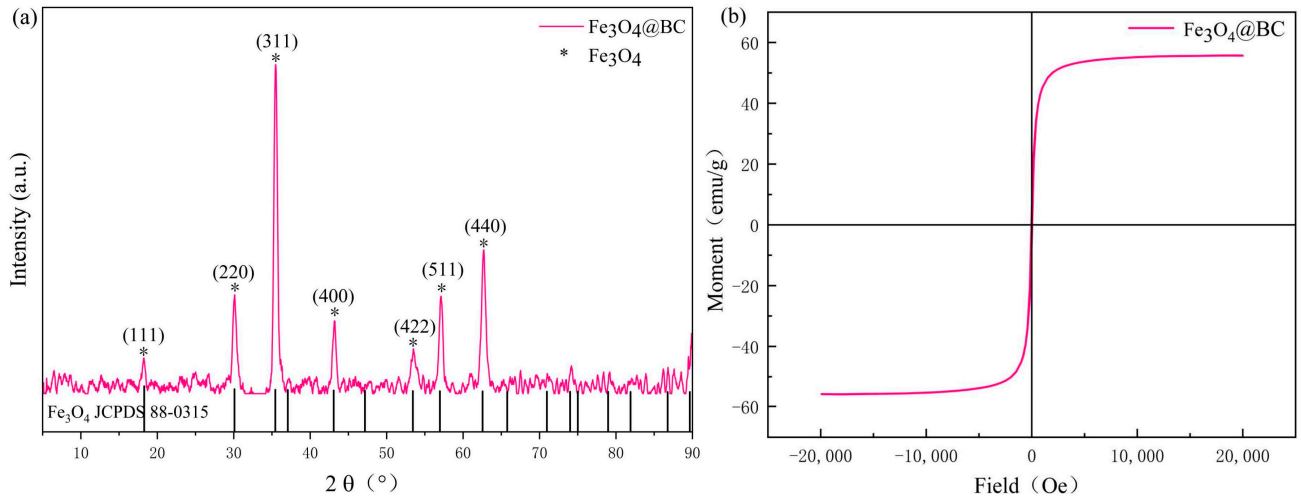

Figure 5. (**a**) XRD patterns of the Fe_3O_4@BC nanospheres samples; (**b**) magnetic hysteresis loops of Fe_3O_4@BC nanospheres samples.

The further verification of the functional groups present in the Fe_3O_4@BC composite was conducted through FT-IR analysis (Figure 6). The spectra revealed several key functional groups, each of which may play a pivotal role in the composite's performance during anaerobic fermentation and its ability to support DIET. The peak at 572.8 cm^{-1} is attributed to Fe-O stretching, confirming the Fe_3O_4 in the composite. This functional group is essential for facilitating electron transfer processes, particularly in the AD environment [21]. The peak at 1016.4 cm^{-1} is indicative of C-O stretching vibrations, likely corresponding to hydroxyl (–OH) or ether (C–O–C) functional groups. These groups, commonly present on BC, may contribute to the surface reactivity and microbial interactions within the composite [22]. The peak at 1620.1 cm^{-1} is characteristic of C = O stretching vibrations, which may arise from carboxyl (–COOH) or carbonyl (C = O) groups [23]. These functional groups are known to be highly reactive and may participate in microbial interactions or contribute to electron transfer during AD. The peak at 3419.5 cm^{-1} is indicative of O-H stretching vibrations, confirming the presence of hydroxyl groups (–OH), which may play a role in hydrogen bonding, promoting microbial interactions, and enhancing the composite's reactivity in the fermentation environment [24].

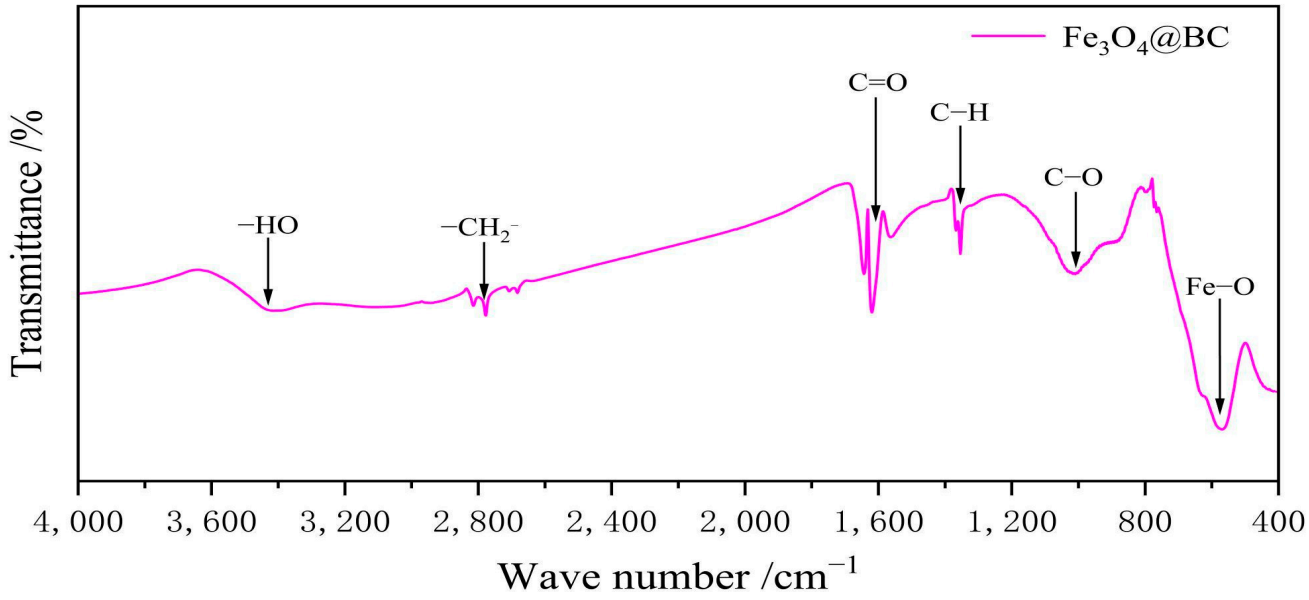

Figure 6. FT-IR spectra of Fe_3O_4@BC.

The microstructure of Fe_3O_4@BC was examined using scanning electron microscope (SEM). As shown in Figure 7a,b, BC appears as irregular particles with a porous surface structure. Fe_3O_4 nanoparticles are attached to the surface of BC and within the pores, exhibiting a clustering phenomenon. These clusters are approximately 200 nm to 800 nm in size. Elemental distribution mapping revealed that the Fe element is uniformly distributed across the surface of BC. Additionally, energy dispersive spectrometry (Figure 7c,d) was used for quantitative analysis of the surface composition. The results showed that the mass percentage of Fe was 68.51%, while the mass percentage of C was 11.70%, confirming the high loading of Fe_3O_4 nanoparticles on the surface of BC.

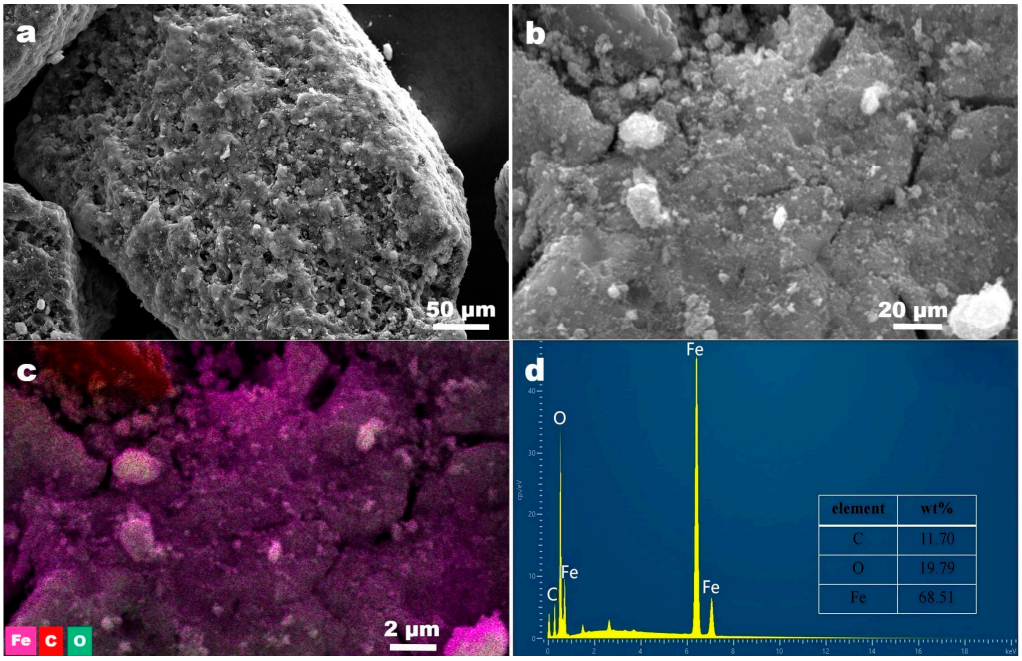

Figure 7. SEM images of the (**a**,**b**) Fe_3O_4@BC; (**c**) energy dispersive spectroscopy (EDS) spectra; (**d**) EDS elemental analysis.

3.2. The Effect of Fe_3O_4@BC Addition Concentration on Gas Production from VW

3.2.1. The Effect of Fe_3O_4@BC on OLR and Gas Production Rate

As illustrated in Figure 8, the fermentation cycle was divided into three distinct stages.

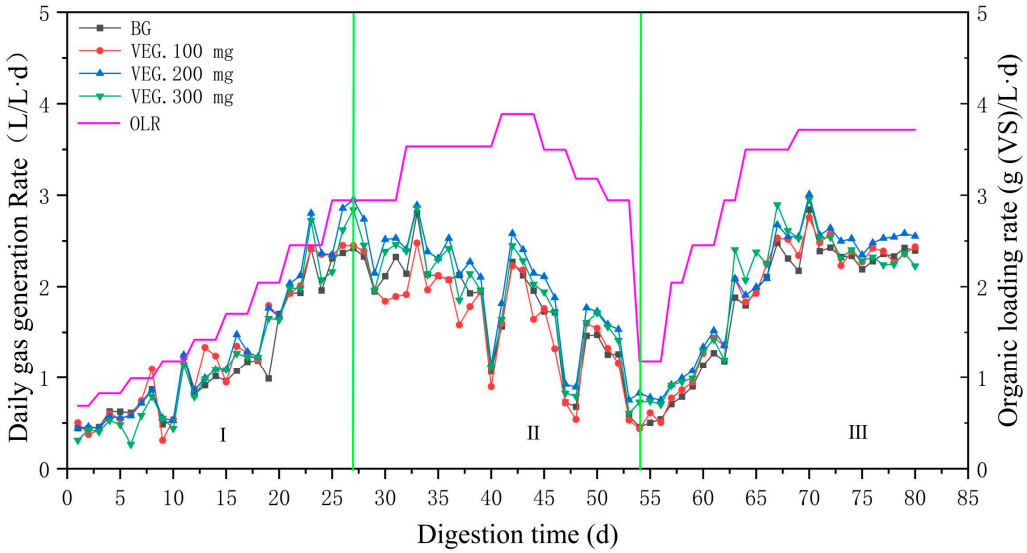

Figure 8. Daily biogas production and OLR of anaerobic fermentation of vegetable waste.

Stage I: Early Phase of Anaerobic Fermentation

In this stage, as the OLR gradually increased, the volumetric gas production rate in the experimental groups exceeded that of the BG. By the 26th day, the AD system reached its maximum fermentation volume of 4.5 L. Afterward, biogas slurry of the same volume was discharged following daily feeding. On the 27th day, the volumetric gas production rates of the experimental groups and BG peaked at 2.951 L/L·d (VEG.200 mg), 2.840 L/L·d (VEG.300 mg), 2.450 L/L·d (VEG.100 mg), and 2.421 L/L·d (BG), respectively, with an OLR of 2.945 g (VS)/L·d.

Stage II: Recovery Period of Anaerobic Fermentation Instability

As the OLR was further increased, a decline in gas production rate was observed. Notably, on the 42nd and 43rd days, when the OLR reached its maximum value of 3.887 g (VS)/L·d, the gas production rate abruptly increased before experiencing a significant decrease. This trend indicated the accumulation of volatile fatty acids (VFAs) in the fermentation system, signaling that the OLR had exceeded the system's tolerance threshold, thereby inhibiting the activity of methanogenic archaea and resulting in a marked reduction in gas production rate. Subsequently, the OLR was reduced rapidly, and the rate of decline in gas production slowed. By the 53rd to 56th days, when the OLR dropped to 1.183 g (VS)/L·d, the gas production rate stabilized. Notably, the VEG.100 mg group exhibited a significant reduction, while the VEG.200 mg group showed a relatively smaller decrease, suggesting that the addition of Fe_3O_4@BC at 200 mg/L offered the best resistance to OLR shock.

Stage III: Final Recovery Period of Anaerobic Fermentation Stability

Beginning on the 57th day, the OLR was gradually increased again. As in the early stage of fermentation, the gas production rate in the experimental groups remained significantly higher than that of the BG. When the OLR reached 3.715 g (VS)/L·d, the gas production rate approached the maximum value previously observed. On the 70th day, the maximum gas production rates were recorded at 3.009 L/L·d (VEG.200 mg), 2.956 L/L·d (VEG.300 mg), 2.757 L/L·d (VEG.100 mg), and 2.844 L/L·d (BG). For the next 12 days, the system maintained a stable gas production rate without significant decline, indicating that the optimal OLR had been reached.

3.2.2. The Effect of Fe_3O_4@BC on Cumulative Biogas Production

As shown in Figure 9, the cumulative total biogas production during the early stage did not exhibit a significant difference between the experimental groups and the BG. However, as the OLR increased, the cumulative biogas production of the VEG.200 mg and VEG.300 mg groups was significantly higher than that of BG, while the difference between VEG.100 mg and BG remained negligible. In the later stage, after the OLR was optimized, the trend in cumulative total biogas production followed the following order: VEG.200 mg > VEG.300 mg > VEG.100 mg > BG.

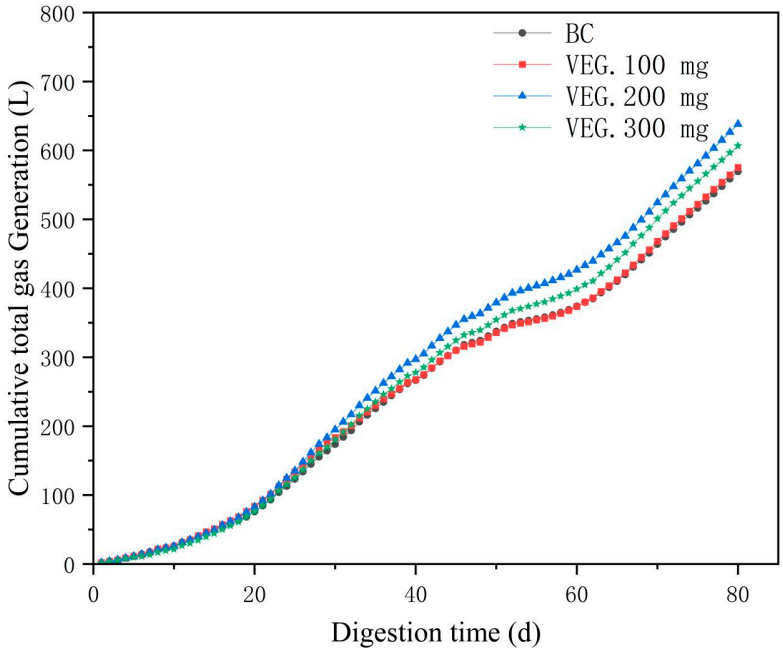

Figure 9. Cumulative total biogas production of VW in different experimental groups.

These results indicate that the addition of Fe_3O_4@BC can effectively enhance biogas production during the anaerobic fermentation of vegetable waste. At an addition concentration of 100 mg/L, Fe_3O_4@BC had a minimal effect on biogas production. In contrast, at higher concentrations (300 mg/L), there was an inhibition of further increases in biogas production. Therefore, the optimal concentration of Fe_3O_4@BC for enhancing biogas production in this fermentation system is 200 mg/L.

This study concludes that the most significant increase in biogas production from the anaerobic fermentation of vegetable waste (VW) was observed when the addition of Fe_3O_4@BC was 200 mg/L and the OLR was 3.715 g (VS)/L·d. Under these conditions, the system achieved an average volumetric gas production rate of 2.57 L/L·d and an average substrate-specific gas production rate of 0.658 L/g (VS). Edwiges et al. [25] evaluated the AD of fruit and VW and determined that the optimal OLR was 3.0 g (VS)/L·d, with a maximum gas production rate of 1.55 L/L·d. Additionally, Liao et al. [26] conducted a study on methane production from AD of Chinese cabbage waste, where the highest gas production rate was reported as 0.480 $L.g^{-1}$ VS^{-1}. These results are substantially lower than the findings of this study, where the OLR of 3.715 g (VS)/L·d, the average volumetric gas production rate of 2.57 L/L·d, and the average raw material gas production rate of 0.658 L/g (VS) highlight the enhanced methane production efficiency. Thus, the increase in OLR and raw material gas production rate in this study can be attributed to the addition of Fe_3O_4@BC, which facilitated the DIET process and promoted methane production efficiency. However, it should be noted that while a small amount of Fe_3O_4@BC had little impact on gas production, excessive amounts of Fe_3O_4@BC could potentially disrupt the cell membrane integrity of methanogenic archaea, thus inhibiting methane production [27].

3.2.3. The Effect of Fe_3O_4@BC on Methane Content

The methane concentration during the experiment is presented in Figure 10a. In the early stage of fermentation, the methane concentration rose rapidly above 50% due to the low OLR of the VW. As the OLR increased, the methane concentration gradually stabilized. Between days 47 and 57, during the recovery phase of anaerobic fermentation instability, the methane concentration decreased. Between days 47 and 57, during the recovery phase of anaerobic fermentation instability, the methane concentration decreased.

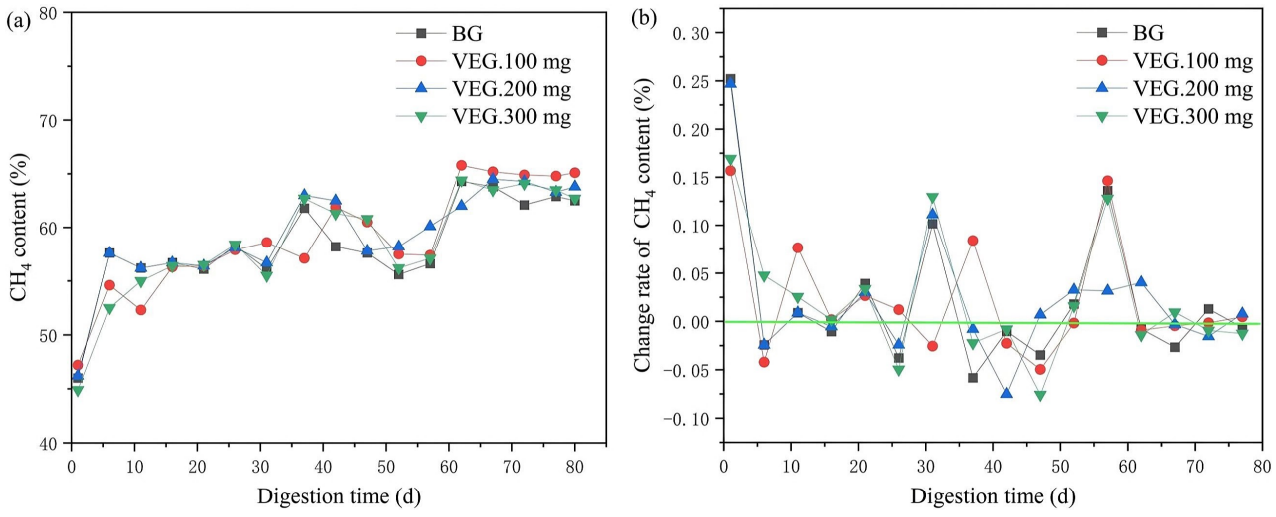

Figure 10. (**a**) Methane content in different experimental groups; (**b**) Change rate of methane content in different experimental groups.

However, during the later stages of the recovery period, as the methane production rate of methanogenic archaea increased, the methane concentration began to rise again, reaching its peak when the OLR was optimized, before stabilizing. Throughout the fermentation process, the peak methane concentration in the VEG.100 mg group was 65.8%, which

was slightly higher than the concentrations in the VEG.200 mg (64.5%), VEG.300 mg (64.4%), and BG (64.3%) groups. While the peak methane concentration in the experimental groups was slightly higher than that of the control group (BG), the difference was not statistically significant.

From the perspective of the entire fermentation cycle, as shown in Figure 10b, the methane concentration change rate in the VEG.200 mg group was relatively smaller compared to the other groups during both the anaerobic fermentation instability and recovery periods. The more stable methane concentration and change rate in VEG.200 mg further suggest that the appropriate addition of Fe_3O_4@BC enhances the stability of the fermentation system and promotes the growth and activity of methanogenic archaea. This indicates that Fe_3O_4@BC supports the stability and efficiency of methane production in the AD process.

3.2.4. The Effect of Fe_3O_4@BC Addition Concentration on VFAs of VW

Throughout the entire anaerobic fermentation process, the pH value ranged from 6.89 to 7.94 (Figure 11a), with an average of 7.5 ± 0.2. Despite the gradual increase in OLR and the system experiencing instability from days 40 to 53, the pH did not significantly decrease or become acidic. In general, the pH in the BG group was lower than that in the experimental groups.

The trend in volatile fatty acids (VFAs) is shown in Figure 11b. The data for each group, from left to right, are BG, VEG.100 mg, VEG.200 mg, and VEG.300 mg, and the VFAs initially increased before decreasing in the early stages of fermentation. A significant increase in VFAs was observed on day 45, especially a sharp rise in butyric acid concentration. The hydrolyzed products of vegetable waste primarily consist of acetic acid and butyric acid, with acetic acid accounting for approximately 43% and butyric acid accounting for about 40% [28]. Due to the positive Gibbs free energy in the degradation of butyric acid, it tends to accumulate during high-load AD, which can lead to reactor instability. In the early stage, propionic acid and butyric acid were the main components of VFAs. However, in the later stage, while the butyric acid concentration decreased significantly, the propionic acid content remained relatively unchanged, constituting about 50%. Previous studies by Edwiges et al. [25] and Shen et al. [29] also reported that in AD of fruit and vegetable waste, the accumulation of VFAs was primarily in the form of propionic acid.

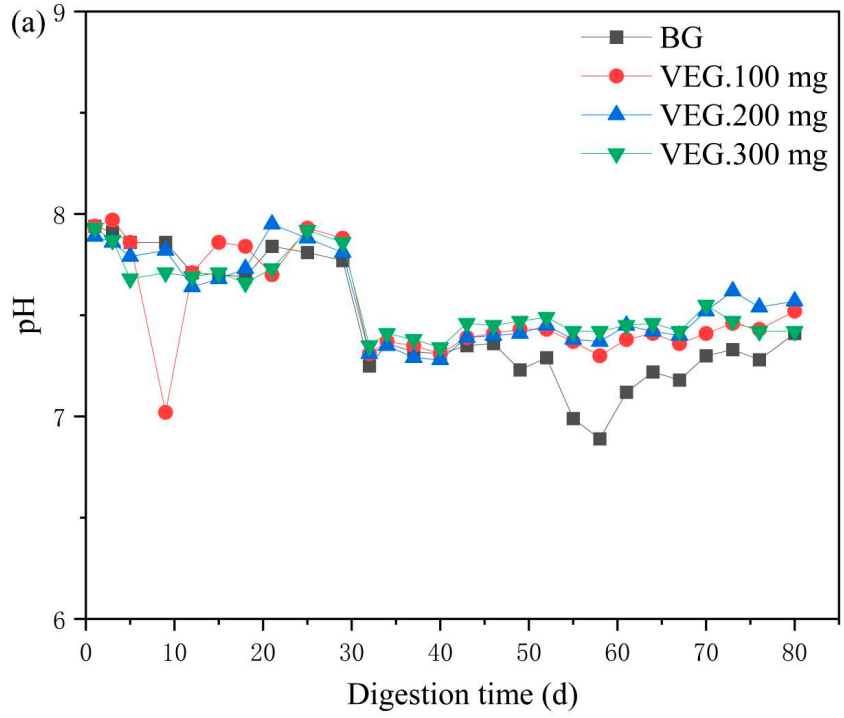

Figure 11. *Cont.*

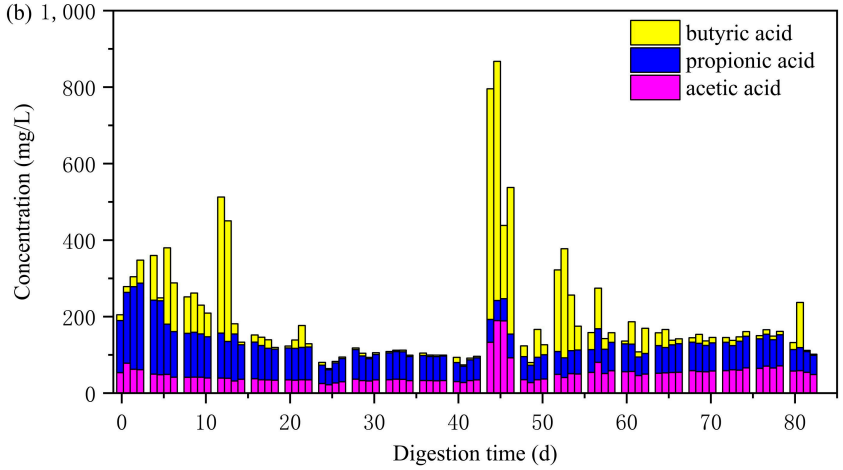

Figure 11. (**a**) pH change graph in different experimental groups; (**b**) VFAs concentration graph in different experimental groups.

Notably, on day 45, Fe_3O_4@BC was replenished. Following the addition of Fe_3O_4@BC, the VFAs decreased significantly, particularly the concentration of butyric acid, indicating that Fe_3O_4@BC contributed to the degradation of butyric acid. This suggests that Fe_3O_4@BC not only supports the stability of the fermentation system but also aids in mitigating the accumulation of inhibitory VFAs, such as butyric acid, thereby improving the overall performance of the AD process.

3.3. The Effect of Fe_3O_4@BC Addition on the Microbial Community Structure of VW

3.3.1. Alpha Diversity Analysis

Diversity indices (Simpson, Shannon), richness indices (Chao1, Ace), and coverage indices (Coverage) were utilized to evaluate the species diversity, richness, coverage, and other information of the microbial communities in the four experimental groups. For both bacterial and archaeal communities, the Coverage values for all four groups were 99%, indicating that the results of this study accurately reflect the microbial community structures in the samples.

As shown in Table 2, after the addition of Fe_3O_4@BC, both Shannon and Simpson indices for bacteria in the VEG.200 mg and VEG.300 mg groups increased compared to the BG group, This suggests that the bacterial communities in these experimental groups exhibited higher diversity. In contrast, the bacterial community diversity in the VEG.100 mg group, which had a lower concentration of Fe_3O_4@BC, decreased. In terms of richness, as indicated by the Chao1 and Ace indices, all experimental groups except VEG.100 mg had higher values than the BG group, demonstrating that the bacterial communities in the VEG.200 mg and VEG.300 mg groups had greater abundance. These results suggest that an appropriate concentration of Fe_3O_4@BC enhances both the diversity and abundance of the bacterial communities in the AD system.

Table 2. Statistical table of bacterial diversity indices in different experimental groups.

Sample	Shannon	Simpson	Chao1	Ace	Coverage
BG	5.65	0.94	485.17	487.52	0.99
VEG.100 mg	5.63	0.95	460.93	463.82	0.99
VEG.200 mg	5.67	0.95	490.68	493.61	0.99
VEG.300 mg	5.90	0.96	498.28	504.49	0.99

As seen in Table 3, the diversity of archaea following the addition of Fe_3O_4@BC was ordered as follows: VEG.100 mg > VEG.200 mg > BG > VEG.300 mg. This indicates that a moderate addition of Fe_3O_4@BC enhances archaeal diversity, whereas an excessive

concentration (VEG.300 mg) negatively impacts archaea diversity. The chao1 and Ace indices for VEG.200 mg were significantly higher than those of other groups, suggesting that an optimal concentration of Fe_3O_4@BC (200 mg/L) is beneficial in improving archaeal abundance.

Table 3. Statistical table of archaeal diversity indices.

Sample	Shannon	Simpson	Chao1	Ace	Coverage
BG	2.22	0.73	14.00	14.00	0.99
VEG.100 mg	2.59	0.79	14.00	14.00	0.99
VEG.200 mg	2.33	0.74	19.00	19.19	0.99
VEG.300 mg	2.14	0.68	14.00	14.55	0.99

In summary, the results demonstrate that the appropriate addition of Fe_3O_4@BC improves the diversity and abundance of both bacteria and archaea, with a concentration of 200 mg/L yielding the most positive effects on microbial community dynamics. However, excessive Fe_3O_4@BC concentrations may inhibit the growth and diversity of certain microbial populations.

3.3.2. Analysis of Bacterial Biocommunity Structure

The composition and abundance of bacterial communities at the phylum and genus levels in the BG and Fe_3O_4@BC experimental groups with different concentrations are presented in Figure 12. At the phylum level, the dominant groups are *Bacteroidota*, *Firmicutes*, *Cloacimonadota*, *Patescibacteria*, *Synergistota*, and *Spirochaetota*, which together account for more than 90% of the total abundance.

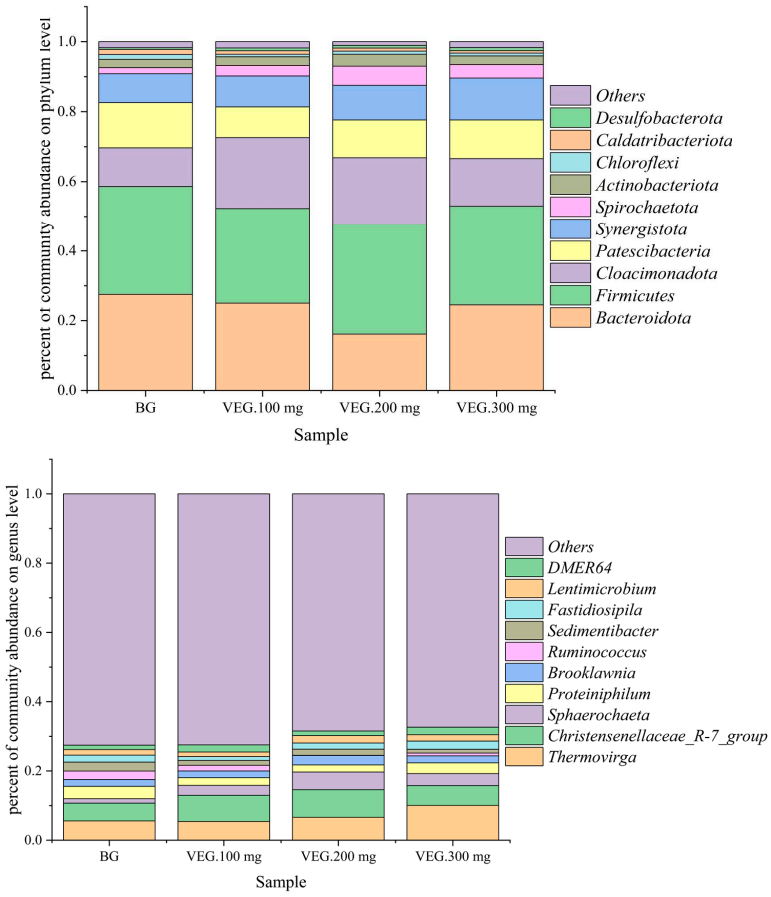

Figure 12. The abundance of bacterial communities at phylum and genus levels in different experimental groups.

Among these, *Bacteroidota* plays a key role in degrading complex organic compounds, such as sugars, cellulose, amino acids, and organic acids, into acetic acid, which serves as a substrate for acetic acid-trophic methanogens [30]. In the BG group, *Bacteroidota* accounted for 27.53%, while in the VEG.200 mg group, its abundance decreased to 16.14%. This reduction suggests that the addition of Fe_3O_4@BC inhibits the growth and reproduction of *Bacteroidota*, thereby slowing the hydrolysis of cellulose and the production of VFAs. This effect can help prevent the rapid accumulation of VFAs during the fermentation of VW, thus stabilizing the fermentation process.

The *Cloacimonadota phylum* is also significant in cellulose hydrolysis, and studies have demonstrated a positive correlation between its abundance and biogas production [31]. For example, Wei et al. [32] found that although *Cloacimonadota* accounted for less than 1.5% of the microbial community, it played a crucial role in the hydrolysis and acidification processes of the substrate. Similarly,Yang et al. [33] observed that in co-digestion systems, the abundance of *Cloacimonadota* was positively correlated with methane production. The addition of Fe_3O_4@BC significantly increased the abundance of *Cloacimonadota* in the experimental groups, further supporting the positive relationship between the abundance of this phylum and gas production, as indicated in Figure 8.

At the genus level, the three most abundant species were *Thermovirga*, *Christensenellaceae*_R-7_group, and *Sphaerochaeta*. *Thermovirga* is known for its strong hydrolytic and sulfate-reducing abilities, which contribute to the breakdown of complex organic compounds [34]. The *Christensenellaceae*_R-7_group is involved in cellulose degradation and provides carbon sources for microbial growth, while *Sphaerochaeta* plays a role in both methane production and cellulose degradation [9,11,31]. The addition of Fe_3O_4@BC significantly enhanced the abundance of these three genera, particularly *Christensenellaceae*_R-7_group and *Sphaerochaeta* in the VEG.200 mg group. This suggests that Fe_3O_4@BC promotes the growth of microorganisms that are important for substrate degradation and methane production.

These findings underscore the beneficial effects of Fe_3O_4@BC addition in enhancing microbial diversity and abundance, particularly species involved in methane production and cellulose degradation. The increase in the abundance of specific phyla and genera further supports the positive impact of Fe_3O_4@BC on the anaerobic fermentation process of vegetable waste.

3.3.3. Analysis of Archaeal Biocommunity Structure

During the AD process, the final methane production stage is entirely driven by the archaeal community. Figure 13 shows the abundance of archaeal communities at both the phylum and genus levels. At the phylum level, the dominant groups are *Synergistota*, *Halobacterota*, and *Bacteroidota*, which together account for more than 99% of the total abundance in the AD of VW.

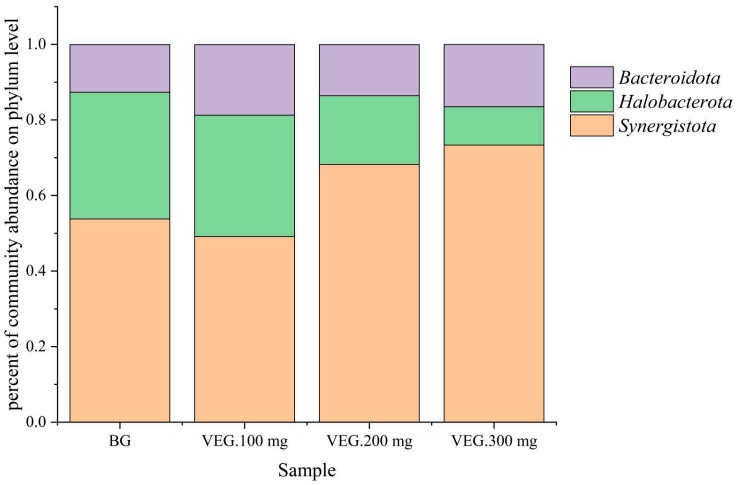

Figure 13. *Cont.*

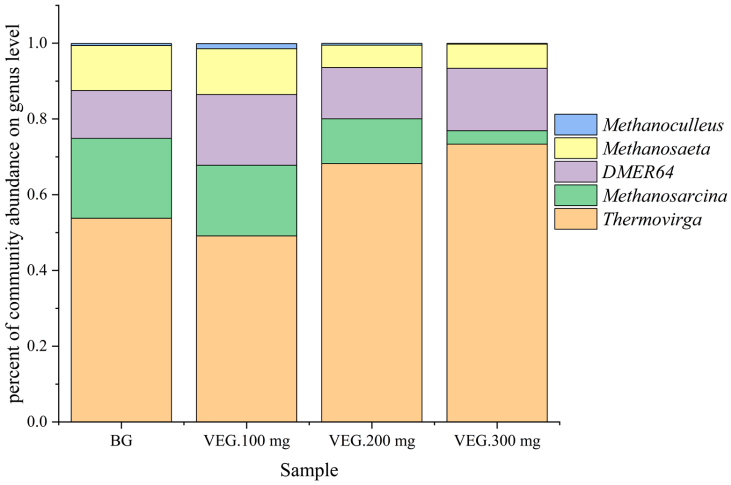

Figure 13. The abundance of archaeal communities at phylum and genus levels in different experimental groups.

In both the BG group (53.77%) and the VEG.200 mg group (68.23%), *Synergistota* was the most abundant phylum. *Synergistota* is a hydrogen-producing and acetic acid-producing group of bacteria that utilizes amino acids as substrates to produce hydrogen and acetic acid. These processes play a crucial role in balancing acid production and methane production in anaerobic digestion [35,36]. Zhao et al. [37] found that in systems with added granular activated carbon, *Synergistaceae* can use amino acids as substrates and leverage granular activated carbon as an electron conductor for DIET to methanogens. The addition of Fe_3O_4@BC significantly increased the abundance of *Synergistota* in the anaerobic fermentation system, suggesting that Fe_3O_4@BC serves as an effective electrical connection to promote DIET between *Synergistota* and methanogens, enhancing the overall methane production efficiency.

At the genus level, the three most abundant genera were *Thermovirga*, *Methanosarcina*, and *Methanosaeta*, which together account for over 99% of the archaeal community. *Thermovirga* is notable for its ability to adapt to high-salt environments and its sulfate-reducing capabilities. Liang Zhu [38] demonstrated in studies on the addition of magnetite to sulfate-containing organic wastewater that Fe_3O_4 enhances the growth of *Thermovirga*, further promoting sulfate reduction. Yang et al. [33] found that in systems with biochar addition, *Thermovirga* dominated and likely participated in DIET alongside Methanothrix. In this study, the addition of Fe_3O_4@BC significantly increased the abundance of *Thermovirga*, which can further enhance the DIET process in the AD of VW, facilitating more efficient methane production.

These results suggest that the addition of Fe_3O_4@BC not only increases the abundance of key archaeal genera but also plays a vital role in supporting the microbial interactions that are essential for methane production, particularly through DIET. This supports the hypothesis that Fe_3O_4@BC can serve as an effective electron shuttle, improving the efficiency of AD systems.

4. Conclusions

In this study, nano Fe_3O_4 particles with an inverse spinel structure were successfully synthesized using the coprecipitation method and subsequently incorporated into the porous structure of biochar. Scanning electron microscopy (SEM) analysis revealed that Fe_3O_4 was evenly distributed within the microporous structure of biochar, effectively preventing agglomeration. The saturation magnetization of Fe_3O_4@BC was determined to be 55.75 emu/g, allowing it to be easily recovered via an external electromagnet.

In the continuous stirred tank reactor AD system, used for the treatment of VW, extensive research was conducted to determine the optimal addition concentration of Fe_3O_4@BC. The results indicated that at an addition concentration of 200 mg/L, the system

exhibited strong resistance to organic loading rate (OLR) shocks and remained stable even at a high OLR of 3.715 g (VS)/L·d. This demonstrates that the addition of Fe_3O_4@BC enhances the stability of the anaerobic fermentation process, preventing acidification under high OLR conditions. Under these optimized conditions, the maximum volumetric gas production rate reached 3.009 $L.L^{-1}$ d^{-1}, while the raw material gas production rate was 0.658 L/g (VS), both significantly improving compared to the other experimental groups.

Moreover, microbial community analysis of both the control and experimental groups revealed that the appropriate addition of Fe_3O_4@BC effectively facilitated direct interspecies electron transfer (DIET) during the anaerobic digestion of vegetable waste. This also resulted in an increase in microbial diversity and the abundance of both bacteria and archaea. Notably, the most significant effects were observed at an addition concentration of 200 mg/L, with the *Christensenellaceae*_R-7_group and *Sphaerochaeta* genus of bacteria, as well as the *Thermovirga* genus of archaea, showing substantial increases in abundance.

This study primarily focuses on the AD of VS, yet the methodologies applied can serve as a valuable reference for the AD of other organic substrates, such as livestock and poultry manure or crop residues. Future research will expand on these findings by investigating the role of various nanomaterials as fermentation additives. Specifically, studies will explore how these nanomaterials can enhance DIET, further elucidating the mechanisms through which conductive materials influence DIET. This work aims to improve the overall stability and efficiency of AD systems, ultimately increasing gas production rates while ensuring long-term operational stability.

Author Contributions: Methodology, formal analysis, H.M. Writing—original draft, H.M. and L.C. Data curation, L.C. Investigation, W.G. Resources, W.G., L.W. and J.Z. Writing—review and editing, D.Z. Validation, L.W. and J.Z. All authors have read and agreed to the published version of the manuscript.

Funding: The authors acknowledge the financial support from the Natural Science Foundation of Gansu Province (23JRRA1659), construction project of the scientific and technological innovation platform of Gansu Natural Energy Research Institute (2019PT-01).

Data Availability Statement: The original contributions presented in this study are included in the article. Further inquiries can be directed to the corresponding author.

Conflicts of Interest: Authors Wei Guo, Lei Wang and Jian Zhang are employed by the Lanzhou Xinrong Environmental Energy Engineering Technology Co., Ltd. The remaining authors declare that the research was conducted in the absence of any commercial or financial relationships that could be construed as a potential conflict of interest.

References

1. National Bureau of Statistics of China. Available online: https://www.stats.gov.cn/ (accessed on 11 September 2024).
2. Li, D.; Chen, L.; Liu, X.; Mei, Z.; Ren, H.; Cao, Q.; Yan, Z. Instability mechanisms and early warning indicators for mesophilic anaerobic digestion of vegetable waste. *Bioresour. Technol.* **2017**, *245*, 90–97. [CrossRef] [PubMed]
3. Ozcan, B.E.; Tetik, N.; Aloglu, H.S. Polysaccharides from fruit and vegetable wastes and their food applications: A review. *Int. J. Biol. Macromol.* **2024**, *276*, 134007. [CrossRef] [PubMed]
4. Usmani, Z.; Sharma, M.; Awasthi, A.K.; Sharma, G.D.; Cysneiros, D.; Nayak, S.C.; Thakur, V.K.; Naidu, R.; Pandey, A.; Gupta, V.K. Minimizing hazardous impact of food waste in a circular economy—Advances in resource recovery through green strategies. *J. Hazard. Mater.* **2021**, *416*, 126154. [CrossRef]
5. Viéitez, E.R.; Mosquera, J.; Ghosh, S. Kinetics of accelerated solid-state fermentation of organic-rich municipal solid waste. *Water Sci. Technol.* **2000**, *41*, 231–238. [CrossRef] [PubMed]
6. Ren, Y.; Yu, M.; Wu, C.; Wang, Q.; Gao, M.; Huang, Q.; Liu, Y. A comprehensive review on food waste anaerobic digestion: Research updates and tendencies. *Bioresour. Technol.* **2018**, *247*, 1069–1076. [CrossRef] [PubMed]
7. Yao, L.; Wang, Y.; Li, R.; Fu, L.; Liu, Z.; Gao, X. Effects of Total Solid Content on Anaerobic Fermentation Performance and Biogas Productivity of Tail Vegetables. *Fermentation* **2024**, *10*, 437. [CrossRef]
8. Hegde, S.; Trabold, T.A. Anaerobic Digestion of Food Waste with Unconventional Co-Substrates for Stable Biogas Production at High Organic Loading Rates. *Sustainability* **2019**, *11*, 3875. [CrossRef]
9. Alvarez, R.; Lidén, G. Semi-continuous co-digestion of solid slaughterhouse waste, manure, and fruit and vegetable waste. Renew. *Energy* **2008**, *33*, 726–734. [CrossRef]

10. Wang, L.; Shen, F.; Yuan, H.; Zou, D.; Liu, Y.; Zhu, B.; Li, X. Anaerobic co-digestion of kitchen waste and fruit/vegetable waste: Lab-scale and pilot-scale studies. *Waste Manag.* **2014**, *34*, 2627–2633. [CrossRef]
11. Baek, G.; Kim, J.; Kim, J.; Lee, C. Role and Potential of Direct Interspecies Electron Transfer in Anaerobic Digestion. *Energies* **2018**, *11*, 107. [CrossRef]
12. Vian, J.; Velasco-Pérez, A.; Solar-González, R.; García-Herrera, T.; Puebla, H.; Vivar-Vera, G. Particle Size Effect on Anaerobic Digestion of Fruit and Vegetable Waste. *Fermentation* **2024**, *10*, 485. [CrossRef]
13. Zhao, Z.; Li, Y.; Zhang, Y. Direct interspecies electron transfer in anaerobic digestion: Research and technological application. *Chin. Sci. Bull.* **2020**, *65*, 2820–2834. [CrossRef]
14. Hou, Y.; Qiu, Q.; Liu, Y.; Huang, W.; Yi, X.; Yang, F.; Lei, Z.; Huang, W. Comparing the effects of magnetite-mediated direct interspecies electron transfer with biogas mixing-driven interspecies hydrogen transfer on anaerobic digestion. *Chemosphere* **2024**, *361*, 142416. [CrossRef]
15. Zhu, Y.; Zhao, Z.; Yang, Y.; Zhang, Y. Dual roles of zero-valent iron in dry anaerobic digestion: Enhancing interspecies hydrogen transfer and direct interspecies electron transfer. *Waste Manag.* **2020**, *118*, 481–490. [CrossRef] [PubMed]
16. Summers, Z.M.; Fogarty, H.E.; Leang, C.; Franks, A.E.; Malvankar, N.S.; Lovley, D.R. Direct Exchange of Electrons Within Aggregates of an Evolved Syntrophic Coculture of Anaerobic Bacteria. *Science* **2010**, *330*, 1413–1415. [CrossRef] [PubMed]
17. Kato, S.; Hashimoto, K.; Watanabe, K. Microbial interspecies electron transfer via electric currents through conductive minerals. *Proc. Natl. Acad. Sci. USA* **2012**, *109*, 10042–10046. [CrossRef]
18. Li, Q.; Xu, M.; Wang, G.; Chen, R.; Qiao, W.; Wang, X. Biochar assisted thermophilic co-digestion of food waste and waste activated sludge under high feedstock to seed sludge ratio in batch experiment. *Bioresour. Technol.* **2018**, *249*, 1009–1016. [CrossRef]
19. Bird, L.J.; Bonnefoy, V.; Newman, D.K. Bioenergetic challenges of microbial iron metabolisms. *Trends Microbiol.* **2011**, *19*, 330–340. [CrossRef] [PubMed]
20. Hong, Y.; Shi, H.; Shu, X.; Zheng, Y.; Zhang, Y.; Wu, Y. Controlled synthesis of hollow magnetic Fe3O4 nanospheres: Effect of the cooling rate. *Particuology* **2017**, *33*, 24–28. [CrossRef]
21. Wei, Y.; Xie, W.; Wang, X.; Chong, Q.; Li, S.; Chen, Z. Photothermal degradation of triphenylmethane dye wastewater by Fe3O4@C-laccase. *Int. J. Biol. Macromol.* **2024**, *282*, 137053. [CrossRef]
22. Zhuang, Z.; Liu, Y.; Wei, W.; Shi, J.; Jin, H. Preparation of biochar adsorption material from walnut shell by supercritical CO2 pretreatment. *Biochar* **2024**, *6*, 11. [CrossRef]
23. Zhao, M.; Zhong, S.; Zhou, X.; Yu, Z. Biochar derived from animal and plant facilitates synergistic transformation of heavy metals and phosphorus in sewage sludge composting. *Environ. Pollut.* **2024**, *357*, 124396. [CrossRef]
24. Pan, F.; Wei, H.; Huang, Y.; Song, J.; Gao, M.; Zhang, Z.; Teng, R.; Jing, S. Phosphorus adsorption by calcium chloride-modified buckwheat hulls biochar and the potential application as a fertilizer. *J. Clean. Prod.* **2024**, *444*, 141233. [CrossRef]
25. Edwiges, T.; Frare, L.M.; Lima Alino, J.H.; Triolo, J.M.; Flotats, X.; Silva de Mendonça Costa, M.S. Methane potential of fruit and vegetable waste: An evaluation of the semi-continuous anaerobic mono-digestion. *Environ. Technol.* **2020**, *41*, 921–930. [CrossRef]
26. Liao, C.; Li, K.; Wang, C.; Liang, C.; Zhao, X.; Wu, K.; Yang, B.; Yin, F.; Zhang, W. Potential and Characteristics of Methane Production During Anaerobic Digestion of Cabbage Waste at Different Temperatures. *BioEnergy Res.* **2023**, *16*, 2549–2559. [CrossRef]
27. Xiu, Z.-m.; Gregory, K.B.; Lowry, G.V.; Alvarez, P.J.J. Effect of Bare and Coated Nanoscale Zerovalent Iron on tceA and vcrA Gene Expression in *Dehalococcoides* spp. *Environ. Sci. Technol.* **2010**, *44*, 7647–7651. [CrossRef] [PubMed]
28. Dinh, P.V.; Fujiwara, T. Biogas Production and Energy Balance in a Two-Stage Anaerobic Digestion of Fruit and Vegetable Waste: Thermophilic versus Mesophilic. *Fermentation* **2023**, *9*, 601. [CrossRef]
29. Shen, F.; Yuan, H.; Pang, Y.; Chen, S.; Zhu, B.; Zou, D.; Liu, Y.; Ma, J.; Yu, L.; Li, X. Performances of anaerobic co-digestion of fruit & vegetable waste (FVW) and food waste (FW): Single-phase vs. two-phase. *Bioresour. Technol.* **2013**, *144*, 80–85. [CrossRef]
30. Park, J.; Cayetano, R.D.A.; Kim, G.-B.; Jo, Y.; Kwon, Y.; Lei, Z.; Kim, S.-H. Sludge disintegration and anaerobic digestion enhancement by alkaline-thermal pretreatment: Economic evaluation and microbial population analysis. *Bioresour. Technol.* **2022**, *346*, 126594. [CrossRef]
31. Alcántara-Hernández, R.J.; Taş, N.; Carlos-Pinedo, S.; Durán-Moreno, A.; Falcón, L.I. Microbial dynamics in anaerobic digestion reactors for treating organic urban residues during the start-up process. *Lett. Appl. Microbiol.* **2017**, *64*, 438–445. [CrossRef] [PubMed]
32. Wei, Y.; Wachemo, A.C.; Yuan, H.; Li, X. Enhanced hydrolysis and acidification strategy for efficient co-digestion of pretreated corn stover with chicken manure: Digestion performance and microbial community structure. *Sci. Total Environ.* **2020**, *720*, 137401. [CrossRef] [PubMed]
33. Yang, S.; Chen, Z.; Wen, Q. Impacts of biochar on anaerobic digestion of swine manure: Methanogenesis and antibiotic resistance genes dissemination. *Bioresour. Technol.* **2021**, *324*, 124679. [CrossRef] [PubMed]
34. Tang, T.T.; Li, J.; Yang, Z.; Luo, X.Y.; Chen, Y. Effect of straw on microbial community composition and degradation efficiency of polycyclic aromatic hydrocarbons in sludge digester. *Int. J. Environ. Sci. Technol.* **2019**, *16*, 7973–7986. [CrossRef]
35. Zou, H.; Chen, Y.; Shi, J.; Zhao, T.; Yu, Q.; Yu, S.; Shi, D.; Chai, H.; Gu, L.; He, Q.; et al. Mesophilic anaerobic co-digestion of residual sludge with different lignocellulosic wastes in the batch digester. *Bioresour. Technol.* **2018**, *268*, 371–381. [CrossRef] [PubMed]

36. Lee, D.H.; Behera, S.K.; Kim, J.W.; Park, H.-S. Methane production potential of leachate generated from Korean food waste recycling facilities: A lab-scale study. *Waste Manag.* **2009**, *29*, 876–882. [CrossRef]
37. Zhao, Z.; Li, Y.; Quan, X.; Zhang, Y. Towards engineering application: Potential mechanism for enhancing anaerobic digestion of complex organic waste with different types of conductive materials. *Water Res.* **2017**, *115*, 266–277. [CrossRef] [PubMed]
38. Zhu, L. Study on Methane Production from Sulfate Organic Wastewater Mediated by Magnetite Particles and Its Microbiological Mechanism. Master's Thesis, Nanjing Normal University, Nanjing, China, 2022.

Disclaimer/Publisher's Note: The statements, opinions and data contained in all publications are solely those of the individual author(s) and contributor(s) and not of MDPI and/or the editor(s). MDPI and/or the editor(s) disclaim responsibility for any injury to people or property resulting from any ideas, methods, instructions or products referred to in the content.